

See discussions, stats, and author profiles for this publication at: <https://www.researchgate.net/publication/230752846>

Does Solution Viscosity Scale the Rate of Aggregation of Folded Proteins?

ARTICLE *in* JOURNAL OF PHYSICAL CHEMISTRY LETTERS · MAY 2012

Impact Factor: 7.46 · DOI: 10.1021/jz300459n

CITATIONS

6

READS

155

6 AUTHORS, INCLUDING:



Mike Sleutel

Vrije Universiteit Brussel

30 PUBLICATIONS 205 CITATIONS

SEE PROFILE



Weichun Pan

Zhejiang Gongshang University

20 PUBLICATIONS 494 CITATIONS

SEE PROFILE



Dominique Maes

Vrije Universiteit Brussel

103 PUBLICATIONS 1,555 CITATIONS

SEE PROFILE



Peter G Vekilov

University of Houston

168 PUBLICATIONS 5,616 CITATIONS

SEE PROFILE

Does Solution Viscosity Scale the Rate of Aggregation of Folded Proteins?

Mike Sleutel,[†] Alexander E. S. Van Driessche,[‡] Weichun Pan,[§] Erwin K. Reichel,[⊥] Dominique Maes,[†] and Peter G. Vekilov^{*,§,||}

[†]Structural Biology Brussels, Flanders Institute for Biotechnology (VIB), Vrije Universiteit Brussel, Pleinlaan 2, B-1050 Brussel, Belgium

[‡]Laboratorio de Estudios Crystalograficos, IACT, CSIC-U.Granada, P.T. Ciencias de la Salud, Avenida del conocimiento s/n, 18100 Armilla (Granada), Spain

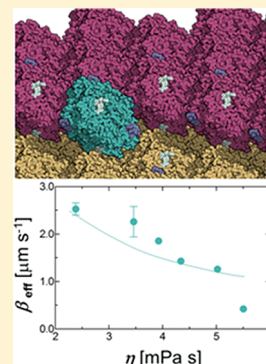
[§]Department of Chemical and Biomolecular Engineering, and ^{||}Department of Chemistry, University of Houston, Houston, Texas 77204, United States

[⊥]Centre for Surface Chemistry and Catalysis, Department of Microbial and Molecular Systems, K.U. Leuven, Kasteelpark Arenberg 23, 3001 Leuven, Belgium

Supporting Information

ABSTRACT: Viscosity effects on the kinetics of complex solution processes have proven hard to predict. To test the viscosity effects on protein aggregation, we use the crystallization of the protein glucose isomerase (gluci) as a model and employ scanning confocal and atomic force microscopies at molecular resolution, dynamic and static light scattering, and rheometry. We add glycerol to vary solvent viscosity and demonstrate that glycerol effects on the activation barrier for attachment of molecules to the crystal growth sites are minimal. We separate the effects of glycerol on crystallization thermodynamics from those on the rate constant for molecular attachment. We establish that the rate constant is proportional to the reciprocal viscosity and to the protein diffusivity. This finding refutes the prevailing crystal growth paradigm and illustrates the application of fundamental kinetics laws to solution crystallization.

SECTION: Biophysical Chemistry and Biomolecules



Protein molecules in properly folded conformations form various aggregates as a part of physiological, pathogenic, laboratory, and industrial processes, e.g., crystals,¹ sickle cell hemoglobin polymers,² eye cataracts,³ and others. In both native and laboratory environments, protein aggregation typically occurs in aqueous solutions. The consequences of the presence of the solvent for the thermodynamics of protein interactions in general and protein aggregation in particular are relatively well understood.^{4–6} While all factors affecting aggregation thermodynamics also influence the rate of aggregation, a unique kinetic factor is the solvent resistance to molecular motion, quantified as viscosity. Viscosity is a macroscopic characteristic of a fluid that describes its resistance to deformation.⁷ Extending Stokes' law to molecular dimensions, Einstein's theory demonstrated that the diffusion coefficient of a solute scaled as reciprocal viscosity.⁸ Kramers' and later theories concluded that in the limit of high friction, the same scaling applied between chemical rate constants and viscosity.^{9–11} In one of the few tests carried out to date of the role of viscosity for the rate of chemical processes, solvent viscosity was found to slow down the rate of protein folding in quantitative agreement with Kramers' theory.^{12,13} However,

other tests revealed that the rates of select enzyme-catalyzed reactions did not depend on solvent viscosity.¹⁴

To test the role of viscosity for the rate of aggregation of folded proteins, we choose the formation of protein crystals as a model for protein aggregation. The lack of in-depth understanding of the biochemical aspects of protein crystallization hampers reliable predictions of the conditions that would lead to crystals of a protein of interest. However, the fundamental physical laws of protein crystal growth are well documented.^{15–17} The majority of protein crystals grow by spreading of layers.^{18,19} The velocity of the edges of the new layers, called steps, quantitatively represents the rate of attachment of protein molecules to the crystal. The step kinetic coefficient β is proportional to the first-order rate constant of attachment of molecules to the surface growth sites.²⁰

In view of the controversial results on the role of viscosity for the rates of solution processes with proteins, a definitive

Received: April 16, 2012

Accepted: April 26, 2012

prediction of the role of viscosity for the kinetics of protein aggregation, including incorporation of molecules into crystals, would be poorly justified. Furthermore, additional controversy related to the step kinetic coefficient β exists: β has been modeled via the vibrational frequency of an activated complex.²¹ This frequency was postulated as inversely proportional to the square root of the molecular mass, as it would be in gas-phase reactions, yielding viscosity-independent β . This model was questioned only recently, when molecular-level data showed that β does not depend on the mass of the crystallizing protein molecules.²² The scaling between the step kinetic coefficient, or the rate constant for protein aggregation, and solvent viscosity has never been tested.

To test the role of viscosity for solution crystallization, we monitor the growth of crystals of the protein glucose isomerase (gluci);²³ for experimental details, see Supporting Information. Gluci crystals are faceted by two families of faces: the {011} prism and {101} dipyrmaid (Figure 1A). Zooming in on areas of a prism face with the confocal microscope (Figure 1B–D), we observe that gluci crystals grow by the spreading of monomolecular layers; this growth mode is present at all supersaturations $(C - C_e)C_e^{-1} < 100$ (C = protein concentration, C_e = solubility).²⁴ The layers are generated either by screw dislocations (Figure 1B and Supplementary Movie I) or by two-dimensional (2D) nucleation (Figure 1C and Supplementary Movie II). Far from the location of step generation, trains of parallel steps form (Figure 1D,E). Since overlapping of the steps' supply fields, either from the solution or from the terraces between them, can retard step motion,²⁵ we monitor only steps separated by distances l greater than $1 \mu\text{m}$ (Figure 1E). In most cases, such noninteracting steps are generated by 2D nucleation.

The rate of incorporation into kinks would be affected by the viscosity at the length scale of the size of the incorporation activated complex, determined by molecules smaller than the protein. Hence, to increase the solvent viscosity, we add glycerol, which is much smaller in size ($\sim 0.6 \text{ nm}$) than gluci ($\sim 9 \text{ nm}$). Glycerol is a common additive in protein crystallization trials²⁶ in which it serves both as a stabilizer and a cryoprotectant.²⁷ We limit the maximum glycerol concentration used to 20 vol %: we observed that higher concentration arrested crystal growth. Figure 1F illustrates that the addition of glycerol strongly retards step motion.

Dynamic light scattering (DLS) determinations (see Supporting Information) of the mean squared displacement $\langle \Delta x^2 \rangle$ of probe particles suspended in the crystallization solution^{29,30} revealed that, for all tested glycerol concentrations, $\langle \Delta x^2 \rangle$ scales as the first power of the delay time in the time range $10^{-4} - 10^{-1} \text{ ms}$. This range includes the characteristic times of gluci diffusion, $0.01 - 0.1 \text{ ms}$, determined independently by DLS (see Supporting Information). The scaling indicates that the hydrodynamic behavior in the crystallization solutions is purely viscous (and not partially elastic^{29,30}) at the relevant time scales, i.e., the solution has a unique viscosity that can be tested for its effects on the aggregation kinetics. Figure 1G shows the solvent viscosity increase associated with the addition of glycerol.

In Figure 2A we display the dependencies of the step velocity v on C at five glycerol concentrations and in the absence of glycerol. Importantly, these dependencies are strictly linear. This linearity indicates the lack of processes whose presence could have complicated the determination of the step kinetic coefficient β , e.g., increase of kink density with supersaturation,

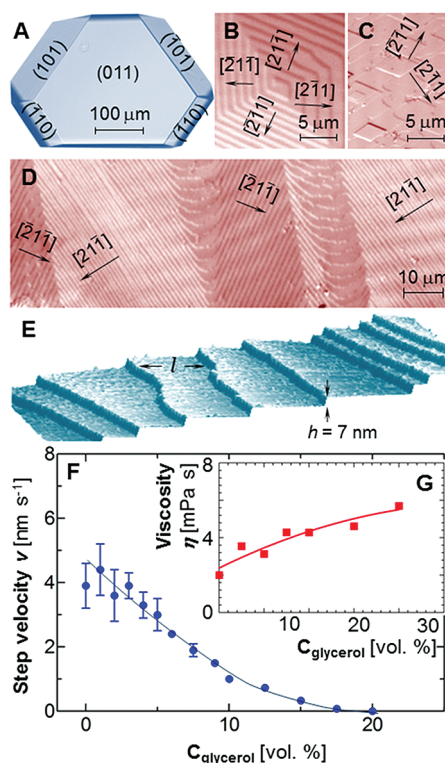


Figure 1. Mechanisms of crystal growth and the overall effect of glycerol on the step motion. (A) Crystal of glucose isomerase imaged by differential interference contrast microscopy; the Miller indexes of the crystal faces are indicated; results on the {011} face are discussed in this paper. (B–D) Scanning confocal microscopy images of a part of the {011} face at gluci concentration $C = 1 \text{ mg mL}^{-1}$ illustrating the generation and propagation of growth steps; the directions of step motion are indicated. (B) The outcrop point of a screw dislocation and a polygonal step spiral emerging from it. (C) Islands generated by 2D nucleation. (D) The pattern of steps generated by several dislocations away from the dislocation outcrop sites. (E) Tapping-mode atomic force microscopy image of a part of a step train at $C = 1 \text{ mg mL}^{-1}$ is displayed in 3D view. Step height $h = 7 \text{ nm}$ and step separation l are indicated. Only steps for which $l > 1 \mu\text{m}$ on both sides along their length were monitored to minimize the effects of overlapping steps' supply fields on step velocity. These were typically steps generated by 2D nucleation, as in C. Since the ratio of the step velocities in the four directions are fixed,²⁸ only steps in the $[2\bar{1}\bar{1}]$ direction were monitored. (F) The dependence of the step velocity v on concentration of glycerol at $C_{\text{protein}} = 1 \text{ mg mL}^{-1}$; v was determined from the evolution of the locations of the steps in sequences of images similar to those in B–D. (G) The effect of glycerol concentration on the solution viscosity; determination by DLS using latex probe particles with radius 200 nm .

which would lead to a superlinear $v(C - C_e)$ dependence at low supersaturations,^{31,32} or overlapping of the step supply fields, which would lead to a sublinear dependence at higher supersaturations.³³ The $v(C - C_e)$ dependencies fit the kinetic law

$$v = \beta_{\text{eff}} \Omega (C - C_e) \quad (1)$$

where $\Omega = 4.99 \times 10^{-19} \text{ cm}^3$ is the molecular volume and β_{eff} is the effective step kinetic coefficient.

Determination of β_{eff} from the lines in Figure 2A requires data on the solubility C_e . To determine C_e , gluci concentration C was lowered at fixed glycerol concentration under confocal microscopy observation.^{34,35} The step velocity v decreased

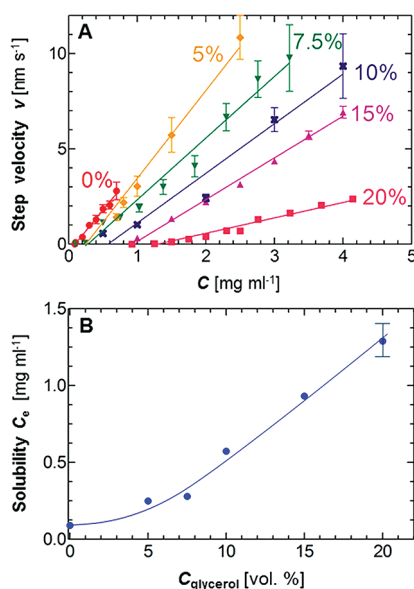


Figure 2. Effects of glycerol on the kinetics and thermodynamics of crystallization of glucose isomerase. (A) Dependencies of the step velocity v on the gluci concentration C at five glycerol concentrations indicated in the plots in volume % and at 0% glycerol. The dependencies cross the C axis at their respective C_e 's. Since these dependencies are linear even at low supersaturation ($C - C_e$), their slope allows determination of the step kinetic coefficient β_{eff} plotted in Figure 4. (B) The dependence of the solubility C_e of the protein determined by observation with scanning confocal microscopy as the lowest concentration at which the growth steps still grow, before retreating at lower concentration. The error in these determinations is 0.1 mg mL^{-1} ; it is equal to the step in the concentration variation and is indicated by the error bar at $C_{\text{glycerol}} = 20 \text{ vol. \%}$.

until, at C_e , the steps fluctuated around a fixed location. At even lower C , the steps retreated. The dependence of C_e on the glycerol concentration is displayed in Figure 2B. Analyses of the crystal packing contacts in the Supporting Information reveal that they are ionic, and glycerol does not partake in them. Hence, the glycerol-induced solubility increase is likely due to its effects on the nonpolar parts of the molecules in the solution.³⁶

The slopes of the lines in Figure 2A allow us to determine β_{eff} . This coefficient contains two contributions: one from the resistance for incorporation at a kink, and the other from the resistance for diffusion toward the steps. The first contribution is accounted for by β . The second contribution is determined by the buoyancy-driven convection, which arises in solutions kept in earth's gravity field owing to the lower density of the partially depleted solution in the vicinity of the crystal.³⁷ The rates of buoyancy-driven convection in the $500 \mu\text{m}$ thick cell are expected to be on the order of $10\text{--}50 \mu\text{m s}^{-1}$.^{38,39} With such flow rates, the width δ of a layer around the crystal, in which the solution is nearly immobile, protein transport is mostly diffusive, and the protein concentration is depleted, is about $50\text{--}100 \mu\text{m}$.^{38,39} The addition of glycerol could slow diffusion through this depleted layer and change its geometry. With this additional resistance, the effective step kinetic coefficient is written as²⁵

$$\beta_{\text{eff}} = (1/\beta + \delta h/Dl)^{-1} \quad (2)$$

where D is the protein diffusion coefficient, and h and l are the step height and interstep distance defined in Figure 1E.

To evaluate the significance of the supply of molecules to the steps, we introduce forced solution flow and determine the dependence of the step velocity on the solution flow rate: forced flow lowers δ .²⁵ At certain fast flow rates, this boundary layer becomes so thin²⁵ that the diffusive resistance becomes negligible, $\delta h/Dl \ll 1/\beta$; further increases of the flow rate do not lead to acceleration of the step velocity. At these fast flow rates, $v = \beta\Omega(C - C_e)$ and $\beta_{\text{eff}} = \beta$. Figure 3 demonstrates that

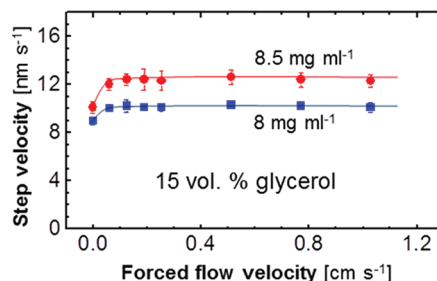


Figure 3. The dependence of the step velocity on the solution flow velocity in the presence of 15 vol % glycerol at the two protein concentrations indicated in the plot.

in the presence of 15 vol % glycerol, at both tested concentrations, forced solution flow accelerates the step velocity by 10–15% compared to the respective values in unstirred solutions. The slightly different diffusive resistance in the two curves in Figure 3 is likely due to the different l 's, corresponding to different step densities caused by varying 2D nucleation rate.²⁸ Similar determinations in the absence of glycerol yielded acceleration due to forced flow by a similar factor. The data in Figure 3 support the general form of eq 2: the diffusive resistance to aggregation becomes vanishingly small at high flow velocities, and step velocity becomes independent of the flow velocity. Equation 2 shows that the diffusive resistance for supply of molecules to the surface scales as D^{-1} and since $D \propto \eta^{-1}$,^{8,40} it is proportional to the solvent viscosity.

Figure 4E,F demonstrates that the effective step kinetic coefficient β_{eff} scales as η^{-1} and is proportional to D for η up to 5 mPa s. Since this scaling is identical to the scaling of the diffusive resistance for the supply of molecules to the surface in eq 2, we conclude that this scaling also applies for β . The value of β_{eff} at the highest glycerol concentration is lower than this trend, and this deviation is likely due to the changes in the geometry of the concentration boundary layer at the higher viscosity of these solutions, which would be reflected in a greater δ .

The contribution of the kinetics at a kink to the step kinetic coefficient β has been modeled, in analogy to the Kramers and Smoluchowski kinetic laws^{9,44} as²²

$$\beta = \frac{D}{\Lambda \bar{n}_k} \exp\left(-\frac{\Delta G^\ddagger}{k_B T}\right) \quad (3)$$

where Λ is the radius of curvature of the potential of interaction between an incoming molecule and a kink at its maximum (usually it is assumed that Λ is equal to the width of two or three water layers, i.e., $\Lambda \approx 1 \text{ nm}$), \bar{n}_k is the mean number of molecules between kinks,^{45,46} ΔG^\ddagger is the free energy barrier for incorporation, k_B is the Boltzmann constant, and T is temperature. The coefficient β relates to the first-order chemical rate constant for incorporation into kinks k as $\beta =$

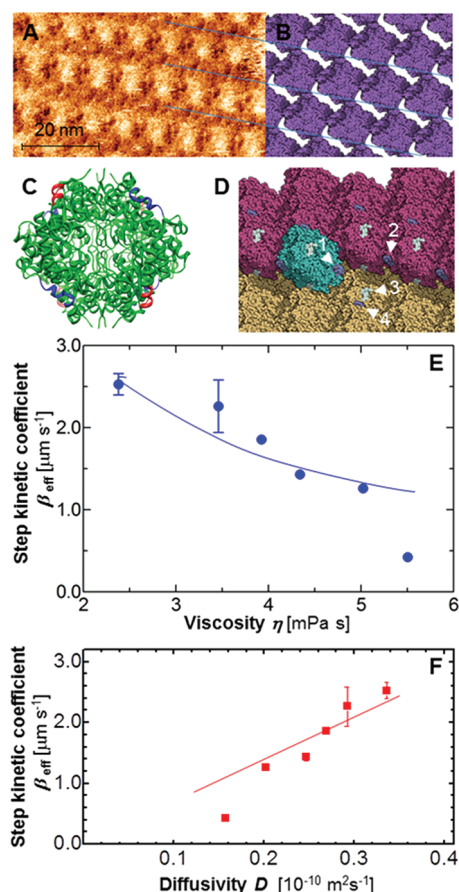


Figure 4. Characterization of the kinetics of incorporation of molecules into steps. (A) Molecular resolution atomic force microscopy image of the surface of the terrace between two steps of a growing crystal of glucose isomerase. (B) The structure of the crystal surface corresponding to Protein Data Base entry 2GLK⁴¹ using package QuteMol 0.4.1⁴² and oriented so that the molecular rows are parallel to those in A. Straight lines highlight the similarity between the surface modeled from the crystal structure and the one experimentally observed by AFM in A. (C) The structure of a gluci molecule corresponding to the same data file as B using the package UCSF Chimera.⁴³ The sites involved in crystal packing contacts are highlighted in red (patch A) and blue (patch B); each crystal contact is a contact between a patch A and a patch B; for the identification of the crystal contacts, see the Supporting Information. (D) Schematic of the incorporation site on a step on a (011) face of a growing glucose isomerase crystal created from the same data file as B and C with the package QuteMol 0.4.1.⁴² The underlying layer is shown in ochre, the growing upper layer is in purple, and a molecule entering the kink is in teal. The contact patches on the molecular surfaces (see the Supporting Information for details) are highlighted in navy (type A) and silver (type B). For a 3D view of the kink, see Supporting Movie III. (E) The dependence of the step kinetic coefficient β on the solution viscosity η ; β was determined from the plots in Figure 2A, η was varied by the addition of glycerol as shown in Figure 1G and determined by DLS. The dashed curve depicts the relation $\beta = \beta(C_{\text{glycerol}} = 0) \eta(C_{\text{glycerol}} = 0)/\eta$. (F) The dependence of the step kinetic coefficient β on the protein diffusion coefficient D . The dashed line depicts the relation $\beta = \beta(C_{\text{glycerol}} = 0) D/D(C_{\text{glycerol}} = 0)$.

$a \cdot k$, where a is the molecular diameter. The analogy of eq 3 to Kramers' formula is apparent upon substituting D for the reciprocal friction coefficient ζ^{-1} and Λ^{-1} for the vibrational frequency at the transition state ω ; \bar{n}_k^{-1} can be viewed as an additional transition state entropy factor. Since $\zeta = 3\pi a\eta$, eq 3

predicts that β , and hence k , scale as η^{-1} . In the derivation of eq 3, the high-friction regime is implicitly accounted for by assuming that molecules entering kinks overcome the energy barrier for incorporation by Brownian diffusion.²²

Our experimentally obtained scaling of β with D is in agreement with eq 3 only if (1) Glycerol does not destabilize the gluci molecules and in this way reduce the effective concentration of potential growth units in the kink vicinity, and (2) ΔG^\ddagger is not affected by glycerol presence and concentration: ΔG^\ddagger could increase as a result of glycerol-enhanced repulsion between the molecules in a kink and an incoming molecule.

Tests of the unlikely scenario that glycerol destabilizes the gluci molecule (glycerol is used as a stabilizer of protein structure in protein crystallography²⁷) by differential scanning calorimetry (DSC; see Supporting Information) reveal that this does not happen at 20 °C, the temperature of the crystallization data.

In the Supporting Information, we also discuss the possibility that glycerol increases the free energy barrier for incorporation ΔG^\ddagger . We show that the lowering of the dielectric permeability ϵ of the solution³⁴ by glycerol is minor and insufficient to explain the complete growth cessation in Figure 1F. We then employ static light scattering (SLS) to characterize the interactions between gluci molecules in the solution as a model for the interactions in a kink. The data in the Supporting Information indicate that the glycerol-induced enhancement of repulsion between the gluci molecules (likely due to strengthening of the hydration layer around the protein molecules³⁶) is mild and does not depend on the concentration of glycerol. Analyses of the contacts between the molecules in the crystal, highlighted in Figure 4A–D, reveal that glycerol does not affect the crystal packing sites and hence the mild enhancement of repulsion reflected in the SLS data is likely due to glycerol interactions with patches on the gluci surface that do not partake in crystal contacts. While, as discussed above, such interactions explain the increased gluci solubility in the presence of glycerol, no effects of glycerol on ΔG^\ddagger are expected.

Returning to eq 3, the relations between β and the parameters on its right-hand side: \bar{n}_k^{-1} , the transition state enthalpy ΔH^\ddagger and entropy $\Delta S^\ddagger = (\Delta H^\ddagger - \Delta G^\ddagger)/T$, and the length Λ , have already been tested.^{17,47} The results presented here demonstrate the role of the diffusivity D and viscosity η and, in this way, complete the definition of β .

In summary, we explore the role of viscosity for the rate of protein aggregation in solution by using protein crystallization as an example of a physically well-understood aggregation process, which can be monitored with molecular and near-molecular resolution by several analytical techniques. We show that the latter scales as reciprocal viscosity and is proportional to the diffusion coefficient. The found dependence of the rate constant on solvent viscosity is likely valid for other processes of protein aggregation and may be for protein binding to surfaces, other proteins, nucleic acids, and other substrates.

Many of the protein aggregation reactions of interest occur in environments with viscoelastic hydrodynamic response, e.g., high concentration protein solutions and the cytosol of life cells.⁴⁸ The respective viscosity is frequency-dependent, and the response of the aggregation rates to its variations may be different from those observed above.^{10,11} Our results, obtained in purely viscous solutions, represent a benchmark for future studies of this response.

■ ASSOCIATED CONTENT

● Supporting Information

Information on the gluci enzyme; experimental details; two movies of the (011) face of a growing gluci crystal showing the two different mechanism of step generation and their propagation: multiple screw dislocation (movie I) and 2D nucleation (movie II); one movie (movie III) showing a 3D view of the incorporation site on a step. This material is available free of charge via the Internet <http://pubs.acs.org>.

■ AUTHOR INFORMATION

Notes

The authors declare no competing financial interest.

■ ACKNOWLEDGMENTS

We thank L. Buts and Y. Sterckx for assistance with the DCS determinations. This work was supported by grants from the PRODEX Program of the European Space Agency (ESA AO-2004-070) to D.M., the Belgium Federal Science Policy Office (DWTC) to the groups from Belgium, and the National Science Foundation (MCB 0843726) and the Norman Hackerman Advanced Research Program (003652-0078-2009) to P.G.V. The participation of A.E.S.V.D. was supported by Ingenio 2010 under project "Factoría Española de cristalización".

■ REFERENCES

- (1) McPherson, A. *Introduction to Macromolecular Crystallography*; John Wiley: Hoboken, NJ, 2009.
- (2) Eaton, W. A.; Hofrichter, J. Sick Cell Hemoglobin Polymerization. In *Advances in Protein Chemistry*; Anfinsen, C. B., Edsall, J. T., Richards, F. M., Eisenberg, D. S., Eds.; Academic Press: San Diego, CA, 1990; Vol. 40; p 63.
- (3) Asherie, N.; Pande, J.; Pande, A.; Zarutskie, J. A.; Lomakin, J.; Lomakin, A.; Ogun, O.; Stern, L. J.; King, J.; Benedek, G. B. Enhanced Crystallization of the Cys18 to Ser Mutant of Bovine Gamma B Crystallin. *J. Mol. Biol.* **2001**, 314, 663.
- (4) Leckband, D.; Israelachvili, J. Intermolecular Forces in Biology. *Q. Rev. Biophys.* **2001**, 34, 105.
- (5) Ball, P. Water as an Active Constituent in Cell Biology. *Chem. Rev.* **2008**, 108, 74.
- (6) Vekilov, P. G.; Feeling-Taylor, A. R.; Yau, S.-T.; Petsev, D. N. Solvent Entropy Contribution to the Free Energy of Protein Crystallization. *Acta Crystallogr., Sect. D* **2002**, 58, 1611.
- (7) Landau, L. D.; Lifshitz, E. M. *Fluid Mechanics (Course of Theoretical Physics Vol. 6)*, 2nd ed.; Translated from Russian by J. B. Sykes and W. H. Reid; Butterworth Heinemann: Boston, 1997.
- (8) Einstein, A. Zur Theorie der Brownschen Bewegung. *Annalen der Physik* **1906**, 19, 371.
- (9) Kramers, H. A. Brownian Motion in a Field of Force and the Diffusion Model of Chemical Reactions. *Physica A* **1940**, 7, 284.
- (10) Fleming, G. R.; Wolynes, P. G. Chemical Dynamics in Solution. *Phys. Today* **1990**, 43, 36.
- (11) Frauenfelder, H.; Wolynes, P. G. Rate Theories and Puzzles of Hemeprotein Kinetics. *Science* **1985**, 229, 337.
- (12) Ansari, A.; Jones, C. M.; Henry, E. R.; Hofrichter, J.; Eaton, W. A. The Role of Solvent Viscosity in the Dynamics of Protein Conformational Changes. *Science* **1992**, 256, 1796.
- (13) Ballew, R. M.; Sabelko, J.; Gruebele, M. Direct Observation of Fast Protein Folding: The Initial Collapse of Apomyoglobin. *Proc. Natl. Acad. Sci. U.S.A.* **1996**, 93, 5759.
- (14) Loveridge, E. J.; Tey, L. H.; Allemann, R. K. Solvent Effects on Catalysis by *Escherichia coli* Dihydrofolate Reductase. *J. Am. Chem. Soc.* **2010**, 132, 1137.
- (15) McPherson, A. *Crystallization of Biological Macromolecules*; Cold Spring Harbor Laboratory Press: Cold Spring Harbor, NY, 1999.
- (16) Vekilov, P. G.; Chernov, A. A. The Physics of Protein Crystallization. In *Solid State Physics*; Ehrenreich, H., Spaepen, F., Eds.; Academic Press: New York, 2002; Vol. 57; pp 1.
- (17) Vekilov, P. G. What Determines the Rate of Growth of Crystals from Solution? *Cryst. Growth Des.* **2007**, 7, 2796.
- (18) Durbin, S. D.; Feher, G. Studies of Crystal Growth Mechanisms of Proteins by Electron Microscopy. *J. Mol. Biol.* **1990**, 212, 763.
- (19) Malkin, A. J.; Kuznetsov, Y. G.; Land, T. A.; DeYoreo, J. J.; McPherson, A. Mechanisms of Growth of Protein and Virus Crystals. *Nat. Struct. Biol.* **1996**, 2, 956.
- (20) While aggregation is described by second-order kinetics laws, the attachment of molecules to crystals is a heterogeneous reaction that follows first-order kinetics.
- (21) Chernov, A. A.; Komatsu, H. Topics in Crystal Growth Kinetics. In *Science and Technology of Crystal Growth*; van der Eerden, J. P., Bruinsma, O. S. L., Eds.; Kluwer Academic: Dordrecht, The Netherlands, 1995; p 67.
- (22) Petsev, D. N.; Chen, K.; Gliko, O.; Vekilov, P. G. Diffusion-Limited Kinetics of the Solution–Solid Phase Transition of Molecular Substances. *Proc. Natl. Acad. Sci. U.S.A.* **2003**, 100, 792.
- (23) Srivastava, P.; Shukla, S.; Choubey, S. K.; V.S., G. Isolation, Purification and Characterization of Glucose Isomerase Enzyme from *Streptomyces* Species Isolated from Parbhani Region. *J. Enzyme Res.* **2010**, 1, 1.
- (24) Sleutel, M.; Maes, D.; Wyns, L.; Willaert, R. Kinetic Roughening of Glucose Isomerase Crystals. *Cryst. Growth Des.* **2008**, 8, 4409.
- (25) Chernov, A. A. *Modern Crystallography III, Crystal Growth*; Springer: Berlin, 1984.
- (26) *Crystallization of Nucleic Acids and Proteins. A Practical Approach*; Ducruix, A., Giege, R., Eds.; IRL Press: Oxford, U.K., 1992.
- (27) Street, T. O.; Bolen, D. W.; Rose, G. D. A Molecular Mechanism for Osmolyte-Induced Protein Stability. *Proc. Natl. Acad. Sci. U.S.A.* **2006**, 103, 13997.
- (28) Sleutel, M.; Willaert, R.; Gillespie, C.; Evrard, C.; Wyns, L.; Maes, D. Kinetics and Thermodynamics of Glucose Isomerase Crystallization. *Cryst. Growth Des.* **2009**, 9, 497.
- (29) Mason, T. G.; Weitz, D. A. Optical Measurements of Frequency-Dependent Linear Viscoelastic Moduli of Complex Fluids. *Phys. Rev. Lett.* **1995**, 74, 1250.
- (30) Pan, W.; Filobelo, L.; Pham, N. D. Q.; Galkin, O.; Uzunova, V. V.; Vekilov, P. G. Viscoelasticity in Homogeneous Protein Solutions. *Phys. Rev. Lett.* **2009**, 102, 058101.
- (31) Chernov, A. A. Protein Crystals and Their Growth. *J. Struct. Biol.* **2003**, 142, 3.
- (32) Georgiou, D. K.; Vekilov, P. G. A Fast Response Mechanism for Insulin Storage in Crystals May Involve Kink Generation by Association of 2D Clusters. *Proc. Natl. Acad. Sci. U.S.A.* **2006**, 103, 1681.
- (33) Land, T. A.; DeYoreo, J. J.; Lee, J. D. An In-Situ AFM Investigation of Canavalin Crystallization Kinetics. *Surf. Sci.* **1997**, 384, 136.
- (34) Sedgwick, H.; Cameron, J. E.; Poon, W. C. K.; Egelhaaf, S. U. Protein Phase Behavior and Crystallization: Effect of Glycerol. *J. Chem. Phys.* **2007**, 127, 6.
- (35) Van Driessche, A. E. S.; Gavira, J. A.; Patiño Lopez, L. D.; Otalora, F. Precise Protein Solubility Determination by Laser Confocal Differential Interference Contrast Microscopy. *J. Cryst. Growth* **2009**, 311, 3479.
- (36) Farnum, M.; Zukoski, C. Effect of Glycerol on the Interactions and Solubility of Bovine Pancreatic Trypsin Inhibitor. *Biophys. J.* **1999**, 76, 2716.
- (37) Onuma, K.; Tsukamoto, K.; Nakadate, S. Application of Real Time Phase Shift Interferometer to the Measurement of Concentration Field. *J. Cryst. Growth* **1993**, 123, 706.
- (38) Pusey, M.; Witherow, W.; Naumann, R. Preliminary Investigation into Solutal Flow about Growing Tetragonal Lysozyme Crystals. *J. Cryst. Growth* **1988**, 90, 105.

- (39) Lin, H.; Rosenberger, F.; Alexander, J. I. D.; Nadarajah, A. Convective–Diffusive Transport in Protein Crystal Growth. *J. Cryst. Growth* **1995**, *151*, 153.
- (40) Berry, P. S.; Rice, S. A.; Ross, J. *Physical Chemistry*, 2nd ed.; Oxford University Press: New York, 2000.
- (41) Katz, A. K.; Li, X.; Carrell, H. L.; Hanson, B. L.; Langan, P.; Coates, L.; Schoenborn, B. P.; Glusker, J. P.; Bunick, G. J. Locating Active-Site Hydrogen Atoms in D-Xylose Isomerase: Time-of-Flight Neutron Diffraction. *Proc. Natl. Acad. Sci.* **2006**, *103*, 8342.
- (42) Tarini, M.; Cignoni, P.; Montani, C. Ambient Occlusion and Edge Cueing to Enhance Real Time Molecular Visualization. *IEEE Trans. Visualization Comput. Graphics* **2006**, *12*, 1237.
- (43) Pettersen, E.; Goddard, T.; Huang, C.; Couch, G.; Greenblatt, D.; Meng, E.; Ferrin, T. UCSF Chimera—A Visualization System for Exploratory Research and Analysis. *J. Comput. Chem.* **2004**, *25*, 1605.
- (44) von Smoluchowski, M. Versuch einer Matematischen Theorie der Koagulationskinetik Kollpider Losungen. *Z. Phys. Chem.* **1918**, *92*, 129.
- (45) Yau, S.-T.; Petsev, D. N.; Thomas, B. R.; Vekilov, P. G. Molecular-Level Thermodynamic and Kinetic Parameters for the Self-Assembly of Apoferritin Molecules into Crystals. *J. Mol. Biol.* **2000**, *303*, 667.
- (46) Yau, S.-T.; Thomas, B. R.; Vekilov, P. G. Molecular Mechanisms of Crystallization and Defect Formation. *Phys. Rev. Lett.* **2000**, *85*, 353.
- (47) Vekilov, P. G.; Galkin, O.; Pettitt, B. M.; Choudhury, N.; Nagel, R. L. Determination of the Transition-State Entropy for Aggregation Suggests How the Growth of Sick Cell Hemoglobin Polymers Can Be Slowed. *J. Mol. Biol.* **2008**, *377*, 882.
- (48) Yamada, S.; Wirtz, D.; Kuo, S. C. Mechanics of Living Cells Measured by Laser Tracking Microrheology. *Biophys. J.* **2000**, *78*, 1736.